

Using Stable Water Isotopes to Evaluate Basin-Scale Simulations of Surface Water Budgets

A. HENDERSON-SELLERS

ANSTO Environment, Sydney, New South Wales, Australia

K. MCGUFFIE

Department of Applied Physics, University of Technology, Sydney, New South Wales, Australia

D. NOONE

PAOS, and CIRES, University of Colorado, Boulder, Colorado

P. IRANNEJAD*

ANSTO Environment, Sydney, New South Wales, Australia

(Manuscript received 4 December 2003, in final form 6 April 2004)

ABSTRACT

Two rare but naturally occurring isotopes of water, $^1\text{H}_2^{18}\text{O}$ and $^1\text{H}^2\text{H}^{16}\text{O}$, are becoming of practical use in diagnosis of climate and earth system model performance. Their value as tracers and validation tools in hydrological subsystems derives from the systematic and different (from each other and from the most abundant water isotope: $^1\text{H}^1\text{H}^{16}\text{O}$) paths and residence times they exhibit as a result of phase change, chemical exchange, and diffusive differentiation. Applications of the simulation of stable isotopic behavior to resolving uncertainty in global climate or earth system models, including river isotopic characterization of basin changes and plant-respired oxygen isotope "tagging," are limited until more basic criteria such as conservation, current mean climate, and capture of observed variability are demonstrated. Here the authors assess the simulation of isotopic fluxes in basin-scale hydrology, focusing on the representation of land surfaces in numerical models as the current mechanism for incorporating water isotopes. They find that surface water budgets are still rather poorly simulated and inadequately constrained at the scale of large basins, yet surface energy partition can be apparently well captured by models with inadequate land surface parameterization. Despite this, simulations of fluxes and reservoirs of the isotopes H_2^{18}O and $^1\text{H}^2\text{H}^{16}\text{O}$ are demonstrated here to have diagnostic utility in evaluating surface energy and water budgets. The hypothesis that aspects of basin water budgets and fluxes are explained and improved by isotopic investigation is demonstrated.

1. Large-basin simulations

The gross water budget of the earth is well simulated in global climate models. However, when different model simulations are applied to future or past climate changes, the details of the basin-scale hydrology differ (e.g., Houghton et al. 2001). As well as continuing to improve gross water flux measurements and use these to test models, there is also an opportunity to evaluate and perhaps improve basin hydrological parameterizations using a novel dataset: stable water isotopes.

* Additional affiliation: University of Tehran, Tehran, Iran.

Corresponding author address: A. Henderson-Sellers, ANSTO Environment, PMB 1, Menai, NSW 2234, Australia.
E-mail: ahssec@ansto.gov.au

a. Why model stable water isotopes?

The most abundant naturally occurring stable isotopes of water of interest as possible validation tools in hydrological simulations are $^1\text{H}_2^{18}\text{O}$ and $^1\text{H}^2\text{H}^{16}\text{O}$. These isotopes have been used to interpret long-term temperature trends since Dansgaard (1964) (e.g., Petit et al. 1999) and their systematic variations in the water cycle as a result of phase change and diffusion-derived isotopic fractionation have also been exploited (e.g., Salati and Vose 1984). Isotopic variability in precipitation is related mainly to the sources of air masses and their evolution while temperature-dependent equilibrium fractionation during evaporation and turbulent scale interactions in the atmospheric boundary layer increase the heavy isotope species in surface waters producing enrichment along evaporation lines below the global

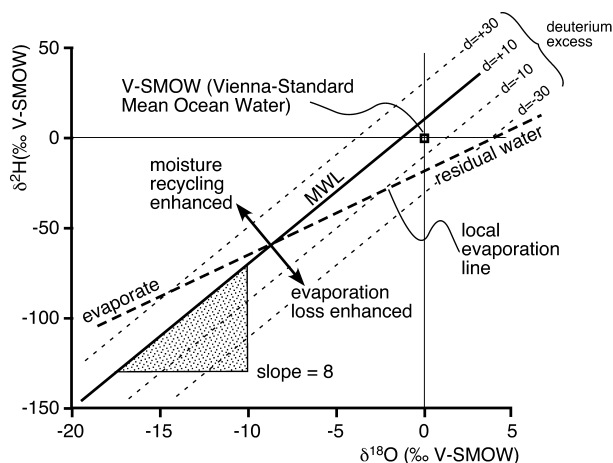


FIG. 1. Schematic of relationships between $\delta^{18}\text{O}$ and δD for various water components of large basins in comparison with the V-SMOW. The slope of eight of the global MWLs is contrasted with the smaller gradient of residual water remaining in lakes and rivers following local evaporation: the local evaporation line. A range of deuterium excess (d) values that show air mass origins and history are also illustrated (redrawn after Froehlich et al. 2002).

meteoric water line (MWL; e.g., Craig 1961; Gat 1996; Fig. 1).

Coupled with measurement of isotopes in water sources, stable water isotope characteristics in river discharge have provided insight into basin-integrated hydroclimates (e.g., Gibson and Edwards 2002). Models of climate change and climatic variability are now being used to project water resources in large catchments, although the more subtle aspects of these simulations of large-basin hydrology still require validation. Features requiring evaluation where isotopes could be applicable include water recycling as a function of precipitation variability, evaporation sourcing (i.e., whether water vapor comes from transpiration or from evaporation from rivers, soil water, wetlands, lakes, or the vegetation canopy), and groundwater recharge/discharge processes including snow and glacier meltwater contributions.

Vegetation interaction with water also modifies isotopic ratios in soil water, groundwater, and river discharges. In the Amazon, interception of rainfall by the plant canopy is the source of reevaporated isotopically "enriched" water (e.g., Gat and Matsui 1991; Henderson-Sellers et al. 2002). This process (rainfall is recycled about 3–4 times in the Amazon) causes a lower continental depletion effect in heavy isotopes: 1.5‰ compared to 2‰ $(1000 \text{ km})^{-1}$ in other major continents (Ingraham and Craig 1986). More recently, water isotopes have been recognized as an additional factor in carbon isotopic differentiation and monitoring of biological and abiological sources and sinks of CO_2 and CH_4 (e.g., Peylin et al. 1999). To utilize biological exchange of isotopes on a global scale, modelers must estimate photosynthetic discrimination of ^{18}O , the ox-

xygen isotopic composition of plant and soil water over the continents and soil respiration (Riley et al. 2002).

Although isotope tracer techniques have not been widely employed in continental-scale water budgets—due largely to lack of available isotope data for major components of the gross hydrological cycle, notably river discharge—uncertainty regarding the capability of the approach is reducing and possible applications are being proposed (e.g., Gibson et al. 2002). Improvement of isotope monitoring in rivers may support a wide range of multidisciplinary international programs currently exploring water and energy budget methods and modeling (Matsui et al. 1983; Rozanski et al. 1993). In cold climate basins with substantial contributions from both evaporation and transpiration (e.g., northern Canada and Russia), stable water isotopes offer a means of monitoring the partitioning of these fluxes in the basin-integrated discharge signals (Gibson 2002). In arid or semiarid regions, the evaporative enrichment of stable isotopes can be used to gauge the progressive downstream water loss by evaporation (Stone et al. 2003). The total latent fluxes in humid basins such as the Amazon can be much larger than the isotopically nonfractionating plant-mediated transpiration resulting in evaporative enrichment of atmospheric moisture (Salati et al. 1979; Henderson-Sellers et al. 2002).

b. Applying stable water isotope knowledge

The hypothesis we test here is that aspects of large-basin water budgets and fluxes can be examined using measurements and simulations of stable water isotopes. If correct, isotopic analysis will be able to explain and improve aspects of large-basin hydrological simulations.

In this paper, we focus on simulations of stable water isotopic characteristics in three of the Global Energy and Water Cycle Experiment (GEWEX) Continental-Scale Experiments' (CSEs') basins: the Amazon, the Murray–Darling, and the Mississippi. Application of isotope techniques to the evaluation, and hopefully improvement, of global climate models necessitates combining understanding of numerical parameterization (e.g., Randall 2000; McGuffie and Henderson-Sellers 2004) and isotopic behavior (e.g., Dansgaard 1964; Gat 2000). Here, we cannot explain either discipline in detail but, recognizing the potential synergies, presume a background in both areas. Our goal is to determine the possible value of detailed isotopic measurements in the various components of larger-basin water budgets as a means of future evaluation of large-scale basin modeling. We do this by first examining the conditions for good simulation of isotopic water budgets (section 2) and then considering in which aspects of such simulations stable water isotopes might provide diagnostic value (section 3).

2. Criteria to be satisfied for isotope application to large-basin modeling

Numerical simulations of basin-scale water movement, sinks, and sources have been evaluated for many years using conventional meteorological and hydrological observations. The isotopic signatures of precipitation differ from that of ocean water because heavier molecules (i.e., those containing heavy isotopes) condense into liquid faster than lighter molecules, termed Rayleigh distillation. Thus, heavy water molecules containing ^2H (deuterium, D) and ^{18}O rain out first in coastal areas, leaving the water vapor remaining depleted in these isotopes. As air masses move farther inland and more water condenses and rains out, the isotope enrichment of the precipitation becomes more and more negative, or depleted in the heavy isotopes (e.g., Yonge et al. 1989). Temperature also influences the isotopic composition of rainwater because of preferential “rain out” of heavier isotopes and because fractionation decreases with temperature. In high latitudes and at higher elevations, lower temperatures increase the distillation of heavy isotopes so that ^{18}O and D enrichments in rain and snow become even more negative (Dansgaard 1964).

For water isotopes to have the utility to add information to simulation efforts over and above that from gross water budgets, there are criteria that need to be satisfied prior to their application, particularly the very basic attributes of conservation, capture of the current mean climate state, and representation of observed variability on a wide range of spatiotemporal scales. In this section, we examine how well existing models being applied to isotopic simulation capture aspects of these fundamentals. Specifically, we consider the simulation of the hydrology of three major river basins (the Amazon, the Murray–Darling, and the Mississippi) with two atmospheric general circulation models (AGCMs). The first already incorporates water isotopes [the Melbourne University GCM (MUGCM)] while the second AGCM incorporates a land surface scheme that has since been recoded to include stable water isotopes [here termed Atmospheric Model Intercomparison Project II (AMIP II) model “F”]. Both AGCMs are assessed using results from their AMIP II 17-yr simulations (Gates et al. 1999). We also compare the coupled and offline predictions of water budgets by the land surface scheme, the former without isotopes.

a. The models and the simulation experiments

The Melbourne University GCM is capable of predicting the ^{18}O and D concentrations in precipitation and atmospheric water (Noone and Simmonds 2002). The AGCM, a primitive equation model here configured to have a horizontal resolution of R21 (3.25° latitude \times 5.625° longitude) and with nine layers in the vertical, captures the general circulation adequately (Noone and

Simmonds 1998). The water isotope module traces ^{18}O and D in parallel to normal water following earlier work of Joussaume et al. (1984) and Joussaume and Jouzel (1993) and has been shown to generate plausible predictions of ^{18}O (Noone and Simmonds 2002). The differentiation of the three tracked water isotopes by fractionation and distillation allows tracing of the two rare isotopes through all aspects of the global water cycle. The simple “bucket” soil hydrology and lack of explicit representation of vegetation in this model limits the detail of isotopic exchange that can be considered.

One particular land surface scheme (LSM) has been chosen to allow comparison with 1 of a set of 20 AMIP II simulations (see Henderson-Sellers et al. 2003a). Prognostic variables include vertically resolved soil water, leaf water and vapor in the canopy, reservoirs for snow, water intercepted by the canopy, and runoff. One specific limitation in this model is the lack of prognostic open water and lakes on the landscape. Nonetheless, detailed analysis shows this formulation is capable of accurately capturing diurnal variations at the canopy level and responds well to recharge by infrequent precipitation events. The land surface scheme has been adapted to simulate the isotopic state of all water pools and fluxes as an extension of the site-level isotopic model described by Riley et al. (2002). In contrast to the simple terrestrial water exchanges simulated in MUGCM, an explicit account of multiple water reservoirs in LSM enables analysis of the interplay and partitioning of energy exchange upon which the ecosystem isotopic conditions are ultimately dependent. Here LSM is operated in two modes: offline with water isotopes forced by prescribed atmospheric parameters (ISOLSM) and globally, coupled into AMIP model F but without isotopes (LSM). Noone et al. (2002) combined the ISOLSM with the MUGCM output offline and gained adequately realistic ^{18}O simulations. Here we employ a similar offline technique: the isotopic discrimination is computed relative to the prescribed precipitation (here termed “offsets”), which may be added to $\delta^{18}\text{O}$ and δD of precipitation obtained elsewhere (observations, or GCM output).

We use the AMIP II AGCMs’ simulations because these experiments are very well constrained in terms of experimental design (Gates 1992; Henderson-Sellers et al. 2003a). The AMIP II period (1 January 1979 through 1 March 1996) includes four El Niños (1982/83, 1986/87, 1991/92, and 1994/95) and just two La Niñas (1984/85 and 1988/89) that are prescribed for the AGCMs because sea surface temperatures (together with sea ice concentration, atmospheric composition, and solar radiative forcing) are set from observed values in the AMIP experiments (Gates et al. 1999; see also <http://www-pcmdi.llnl.gov/amip/amiphome.html> and http://www.cpc.ncep.noaa.gov/products/analysis_monitoring/ensostuff/ensoyears.html). As our aim is to identify the overall strengths and weaknesses in models’ simulations of stable water isotopes against a background of imperfect validation data, we do

TABLE 1. Annual surface hydrologic summaries from the AMIP II and MUGCM models together with a variety of estimates of "truth" for the GLS and three basins (— indicates no data available). Wimb/Pr is water imbalance divided by Pr.

| Source | Pr (mm day ⁻¹) | Ev/Pr | Ro/Pr | Wimb/Pr |
|-----------------|----------------------------|-------|-------|---------|
| GLS | | | | |
| GRDC/CMAP | 1.94 | 0.60 | 0.40 | — |
| NCEP-DOE | 2.40 | 0.79 | 0.45 | 0.23 |
| NCEP-NCAR | 2.37 | 0.77 | 0.53 | 0.30 |
| ECMWF | 2.21 | 0.72 | — | — |
| VIC | 2.07 | 0.67 | 0.33 | 0.00 |
| MUGCM | 2.46 | 0.47 | 0.53 | — |
| Model F | 2.28 | 0.68 | 0.32 | 0.01 |
| Av AMIP II | 2.27 | 0.67 | 0.33 | 0.03 |
| Std dev AMIP II | 0.31 | 0.52 | 0.06 | 0.04 |
| Amazon | | | | |
| Source | Pr (mm day ⁻¹) | Ev/Pr | Ro/Pr | Wimb/Pr |
| GRDC/CMAP | 5.00 | 0.39 | 0.61 | — |
| NCEP-DOE | 5.71 | 0.68 | 0.43 | 0.11 |
| NCEP-NCAR | 5.93 | 0.71 | 0.39 | 0.09 |
| ECMWF | 5.38 | 0.59 | — | — |
| VIC | 5.09 | 0.67 | 0.33 | 0.00 |
| MUGCM | 5.26 | 0.39 | 0.61 | — |
| Model F | 5.80 | 0.65 | 0.35 | 0.00 |
| Av AMIP II | 4.97 | 0.67 | 0.34 | 0.02 |
| Std dev AMIP II | 0.68 | 0.07 | 0.05 | 0.05 |
| Murray-Darling | | | | |
| Source | Pr (mm day ⁻¹) | Ev/Pr | Ro/Pr | Wimb/Pr |
| GRDC/CMAP | 1.50 | 0.92 | 0.08 | — |
| NCEP-DOE | 1.53 | 1.17 | 0.15 | 0.32 |
| NCEP-NCAR | 1.21 | 1.20 | 0.03 | 0.22 |
| ECMWF | 1.28 | 1.47 | — | — |
| VIC | 1.50 | 0.86 | 0.14 | 0.00 |
| MUGCM | 2.00 | 0.79 | 0.21 | — |
| Model F | 1.70 | 1.00 | 0.01 | 0.01 |
| Av AMIP II | 1.71 | 0.98 | 0.09 | 0.08 |
| Std dev AMIP II | 0.74 | 0.15 | 0.11 | 0.11 |
| Mississippi | | | | |
| Source | Pr (mm day ⁻¹) | Ev/Pr | Ro/Pr | Wimb/Pr |
| GRDC/CMAP | 1.96 | 0.75 | 0.25 | — |
| NCEP-DOE | 2.23 | 1.01 | 0.24 | 0.25 |
| NCEP-NCAR | 2.34 | 1.03 | 0.22 | 0.25 |
| ECMWF | 1.77 | 1.06 | — | — |
| VIC | 2.18 | 0.72 | 0.28 | 0.00 |
| MUGCM | 2.13 | 0.68 | 0.32 | — |
| Model F | 2.34 | 0.88 | 0.12 | 0.00 |
| Av AMIP II | 2.32 | 0.82 | 0.20 | 0.03 |
| Std dev AMIP II | 0.43 | 0.07 | 0.08 | 0.06 |

not identify the individual AMIP II models mentioned here, except model F.

b. Basin-scale water budget balance and components

Twenty AGCMs participating in the second phase of AMIP II (e.g., Irannejad et al. 2003) are compared with the MUGCM and the land surface products from the reanalyses of the European Centre for Medium-Range Weather Forecasts (ECMWF; Gibson et al. 1997), the National Centers for Environmental Prediction-National Center for Atmospheric Research (NCEP-NCAR; Kistler et al. 2001), the NCEP-DOE (Department of Energy; Kanamitsu et al. 2002), and a global offline land surface simulation variable infiltration capacity

(VIC; Liang et al. 1994). The observations comprise estimated runoff from the Global Runoff Data Center (GRDC; Fekete et al. 2000) and precipitation from the Climate Prediction Center (CPC) Merged Analysis of Precipitation (CMAP; Xie and Arkin 1997). Table 1 lists the precipitation rate (Pr) totals together with its partition into the runoff (Ro) and evapotranspiration rates (Ev) for three major basins and the global land surface (GLS). Runoff is defined as the surface + subsurface + drainage rates.

There is disagreement between all the simulations and the observations at the global scale: the models generate more precipitation than is observed and all except MUGCM partition more into evaporation than observed. In each of the basins, MUGCM predicts the

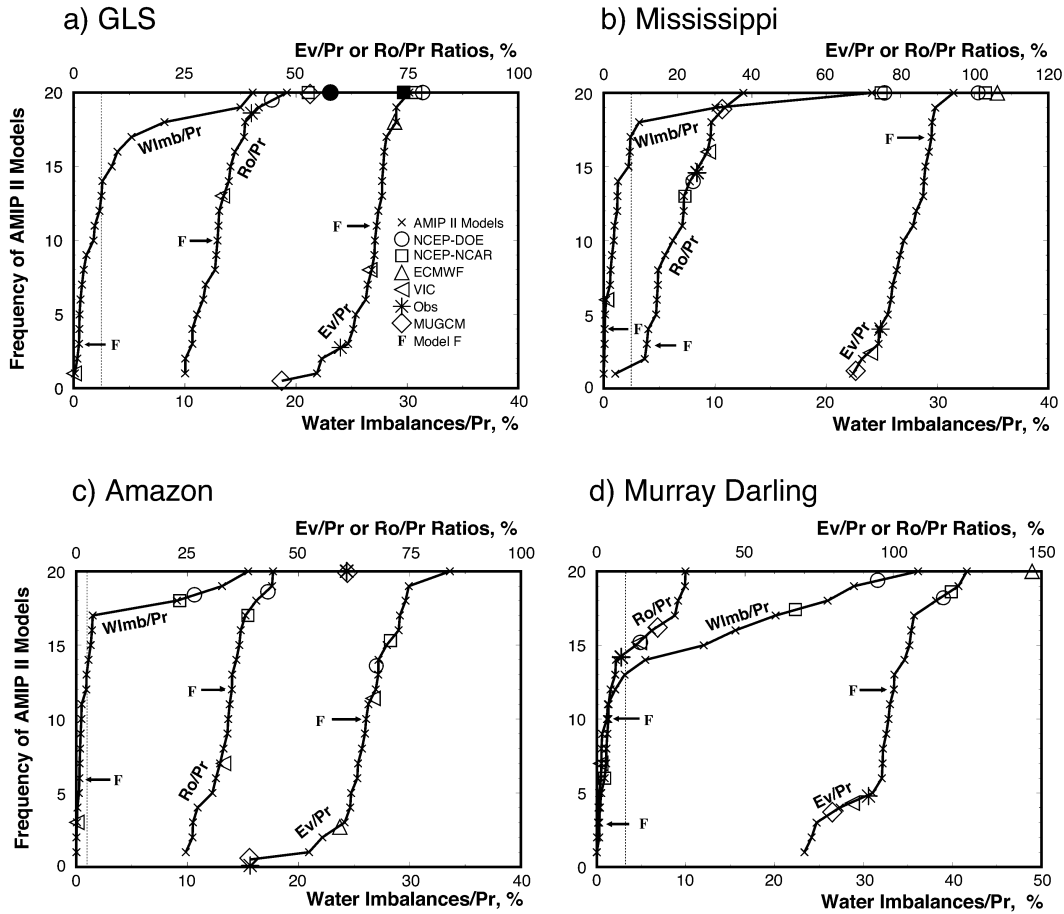


FIG. 2. Frequency distributions from 21 AGCMs: 20 AMIP II models (crosses) and MUGCM (open diamonds), with AMIP model F separately identified by an arrow. The values of 17-yr mean relative water imbalance (Wimb) as a percentage of precipitation $|100/Pr \times dW/dt|$; total (surface + drainage) runoff ratio $100(Ro/Pr)$, and evaporation ratio $100(Ev/Pr)$ are shown in % for the three basins [(b)Mississippi, (c) Amazon, and (d) Murray–Darling] and (a) over the GLS. Observations (based on GRDC runoff and CMAP precipitation: asterisks), reanalyses (NCEP–NCAR: open square; NCEP–DOE: open circle; and ECMWF: open pyramid) and VIC (open left triangle) are included in the figure as symbols. The vertical axis shows the cumulative frequency of the models’ water imbalance (Wimb/Pr), runoff ratio (Ro/Pr), and evaporation ratio (Ev/Pr) and illustrates the position of the evaluation datasets among the models. All horizontal scales are in percentages (of Pr), with the bottom scale being for water imbalance and the top scale for both evaporation and runoff ratios. The faint vertical line shows the “acceptable” margin in the water budget closure of $\pm 0.05 \text{ mm day}^{-1}$ (i.e., simulations with the Wimb/Pr falling to the left of this line are deemed to conserve surface water satisfactorily). For GLS only, the Wimb/Pr points for NCEP–DOE and NCEP–NCAR are solid rather than open for clarity.

smallest Ev/Pr. (Note that the ratio sum often differs from unity; i.e., many models, and especially the reanalyses, fail to conserve water over the continental land surface; e.g., Schlosser et al. 2000).

A basic requirement for any surface water simulation is

$$Pr - Ev - Ro - \frac{dW}{dt} = 0, \quad (1)$$

where dt is the simulation time, and dW is the difference between the final and initial values of the surface water storage (i.e., water stored in the soil, canopy, and as snow and ice on the surface). Although the information needed to calculate dW/dt is not contained in the AMIP

or MUGCM archives, over a long period of time (large dt), the rate of change of the surface water storage in (1) becomes negligible, and hence balance should be achieved between Pr, Ro, and Ev. For the AMIP II simulation, all modeling groups were asked to ensure equilibrium of their continental moisture stores before initiating the 17-yr integration. For these reasons, Henderson-Sellers et al. (2003b) argue that a rate of change in the surface water storage of $\pm 0.05 \text{ mm day}^{-1}$ is acceptable, and, outside this, errors are in conservation and/or due to poor initialization of W (i.e., unrecorded storage changes).

Figure 2 highlights the performance of the two AGCMs examined here [F and MUGCM (open diamond

symbol)] in terms of three fundamental attributes of simulation: (i) the closure of the simulated land surface water budget (WImb/Pr), (ii) the ratio of runoff to precipitation (Ro/Pr), and (iii) the ratio of evaporation to precipitation (Ev/Pr). The frequency distributions are of the 17-yr means of water imbalance, runoff, and evaporation ratios for the GLS and for the Amazon, Mississippi, and Murray–Darling. Reanalyses, VIC (Nijssen et al. 2001), and observations are included in the figure such that the observed runoff ratio is calculated using mean GRDC runoff and CMAP precipitation while the observed evaporation ratio is calculated as the residual from the surface water balance equation assuming a zero rate of change in the surface water. The vertical dotted line shows the assumed acceptable water imbalance threshold value of 0.05 mm day^{-1} as the percentage of the observed precipitation (i.e., simulations conserve water when their relative imbalances appear to the left of this threshold).

Most of the models (16–18 of the AMIP II AGCMs) close the surface water budget to within the margin determined to be acceptable of $\pm 0.05 \text{ mm day}^{-1}$. Figure 2 underlines that globally and within basins, models differ from reanalyses and that the latter can fail to conserve water within the assumed threshold (e.g., in Murray–Darling and the Amazon). The Murray–Darling is the worst simulated basin, with 6 models (out of 17 models with no obvious reporting error) failing to close the water balance to within $\pm 0.05 \text{ mm day}^{-1}$. Also, 7 models implausibly simulate the 17-yr mean evaporation greater than precipitation in the Murray–Darling probably because of poor soil water initialization, despite emphasis on this in the AMIP II protocol. Also in the Murray–Darling (Fig. 2d), a number of AGCMs and some reanalyses simulate mean evaporation greater than precipitation. The AGCMs with $Ev > Pr$ over the entire 17-yr AMIP II experiment exhibit problematically long spinup periods or, worse, fail to conserve water.

Model F, of particular interest here because it uses a variant of the land surface scheme, LSM, examined later, conserves water in every region, although model F reported negative runoff (probably due to a sign error) in the first 2 yr of simulations, so these 2 yr are excluded from these calculations. At the global scale (GLS) the MUGCM performs rather poorly, while model F does adequately well (in the center of the AMIP II predictions). If VIC is taken as the best representation of “truth” then model F does well in the Amazon while MUGCM compares well in the Mississippi and the Murray–Darling. Henderson-Sellers et al. (2003b) argue that VIC (constrained by observed precipitation and tuned for large river flows) provides the most reliable surface water simulation, at least when averaged over a large area and a long period of time (Wood et al. 1998).

In summary, the AMIP II model F successfully closes its surface water budget in all the basins examined and globally (Fig. 2) and appears to perform adequately in its partition of surface available water (Table 1). Al-

though the reported surface water budget is incomplete, the MUGCM seems to behave less well in both aspects of the surface water evaluation at the basin scale. It is fair to add that AMIP II model F and the MUGCM’s representations are no worse than those of the available “truths” against which simulations are traditionally tested (e.g., Henderson-Sellers et al. 2003b; Berg et al. 2003). Nonetheless, there remain many uncertainties and discrepancies in the prediction of large-basin-scale water budgets even when only gross water fluxes are considered. Such variability and clear lack of quantitative understanding increases the value of placing additional (isotopic) constraints on the surface water and energy budgets.

c. Surface water and energy partitioning

The AMIP II models partition available surface energy between sensible heat (SH) and latent heat (LH) such that three groups of land surface schemes (LSSs) appear: an “older” 1- or 2-layer hydrology with no explicit canopy (“no canopy”) (e.g., Manabe 1969), Simple Biosphere (SiB)-based schemes (Sellers et al. 1986) (SiBlings), and a “central” group of current land surface schemes. These results were shown to hold even after excluding the differences due to energy availability by scaling SH and LH against an ensemble of the three available reanalyses (Henderson-Sellers et al. 2003a).

Figure 3 shows that the ranges among the models’ LH and SH are similar in the wet Amazon basin, the midlatitude Mississippi, and the semiarid Murray–Darling basin but slightly reduced for the global average (GLS). The SiBlings compare best with VIC’s LH (vertical arrow in Fig. 3), having small LH and large SH while the 2 layer soil models with no explicit canopy and the bucket models with and without canopy resistance always simulate large LH and small SH. Model F, a current LSS, lies centrally in Fig. 3 while the MUGCM tends toward the SiBlings group everywhere except the Murray–Darling.

While the former result is not surprising because model F’s land surface scheme is, indeed, a fairly complex “big leaf” model, the latter result is unexpected because the MUGCM uses a simple Deardorff-based surface hydrology containing two soil water reservoirs and should, therefore, lie in the group of “no canopy” schemes (e.g., Henderson-Sellers et al. 1995). We believe the reason for this departure is that the upper soil layer depth (12 cm) is so low that the MUGCM continental surface tends to operate close to dryness most of the time despite recharge from the deeper second layer. Generally, the available surface energy must be removed as SH because there is inadequate soil water to allow evaporation. This is particularly clear in the Amazon (LBA in Fig. 3) where the predicted LH is much too low. Overall, the MUGCM behaves well (in the group that performs this partition most accurately), but without a canopy scheme. This may be for the wrong reasons.

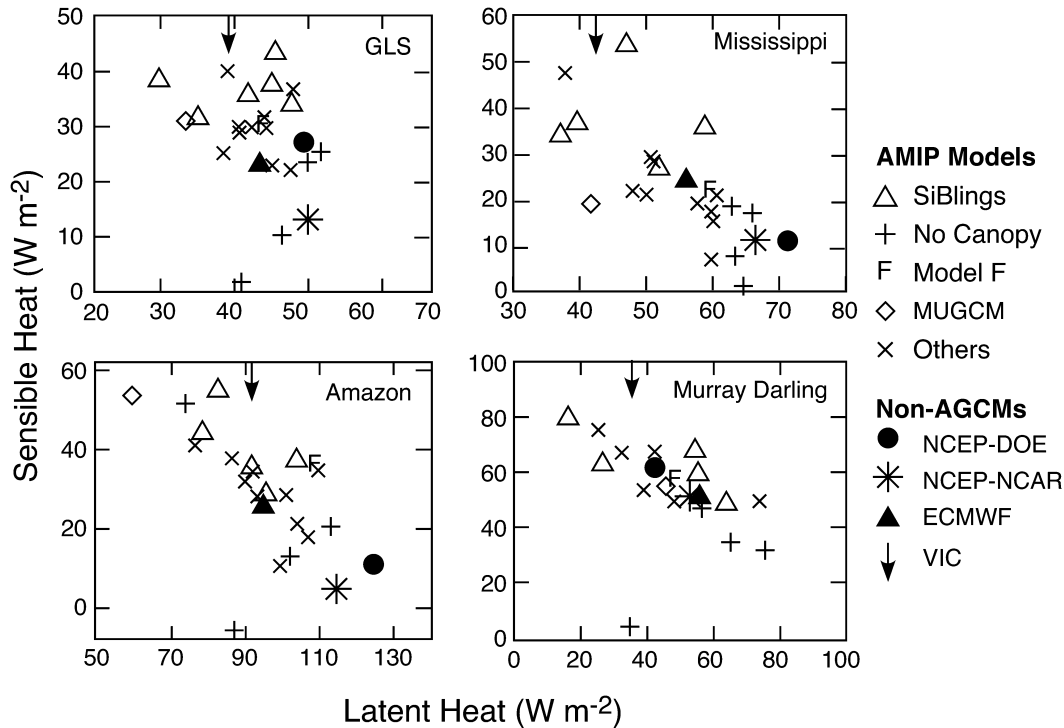


FIG. 3. Partitioning of surface energy between scaled SH and LH for 20 AMIP II AGCMs (shown as three types: SiBlings, No Canopy, and Others, which includes model F), the MUGCM (open diamond), and three reanalyses [NCEP-DOE (asterisk), NCEP-NCAR (solid circle), and ECMWF (solid triangle)] for the GLS and the three basins: Amazon, Murray-Darling, and Mississippi. The vertical downward pointing arrow shows the LH calculated by VIC.

Although there remains significant uncertainty in the prediction of and partition of surface available energy, we find both models evaluated here perform adequately. However, while the simulation by the AMIP II model F is satisfactory, as expected, the MUGCM behaves well for, probably, incorrect reasons. The detected excessive land surface dryness in the MUGCM is likely to affect the simulation of all components of the basins' water budgets and thus possibly modify the behavior of the stable water isotopes. This is investigated in section 3.

d. Seasonal cycle and climatic excursions

Water isotopes are being tested for their ability to provide insights into the complex behaviors of surface water budgets, especially relating to phase state and chemical changes. In order to have confidence in predictions of these, models need to correctly represent current climate conditions and modest excursions from them. Figure 4 shows the seasonal cycle of precipitation and evaporation ratio for the three basins: Amazon, Murray-Darling, and Mississippi. Also shown are the climatic variations caused by the four El Niños and the two La Niñas that occurred during the AMIP II simulation period. In terms of global-scale variability, the Amazon and Murray-Darling should be in phase: both the Murray-Darling and the Amazon are warmer and

drier than average during an El Niño event and cooler and wetter in La Niñas.

The seasonal cycle in precipitation is well captured in all the models of interest here. If VIC is taken to have the most accurate seasonal cycle in evaporation ratio (Irannejad et al. 2003) then this is less well captured by either of the models, particularly in the Murray-Darling and the Mississippi. The NCEP-DOE reanalysis (illustrating the reanalyses) seems to be quite sensitive to ENSO forcing while the AMIP II mean predictions are least responsive to imposed El Niño/La Niña excursions. The latter behavior might be expected from an ensemble average, although it is interesting to note that AMIP II model F also fails to show very large sensitivities to the ENSO signal except perhaps in the Murray-Darling. Indeed, the Murray-Darling basin exhibits the most variability (among models and from month to month) and greatest sensitivity to El Niño/La Niña changes. In the other two basins, the observations (CMAP) and the AMIP II mean are the least variable and least sensitive while the MUGCM has characteristics similar to the NCEP-DOE reanalysis and VIC.

The two models of particular interest demonstrate reasonable simulation of both the seasonal cycle and the representation of El Niño (La Niña) drought (flood) climate extremes. Their water budget climatic excursions around present-day regimes can be simulated satisfac-

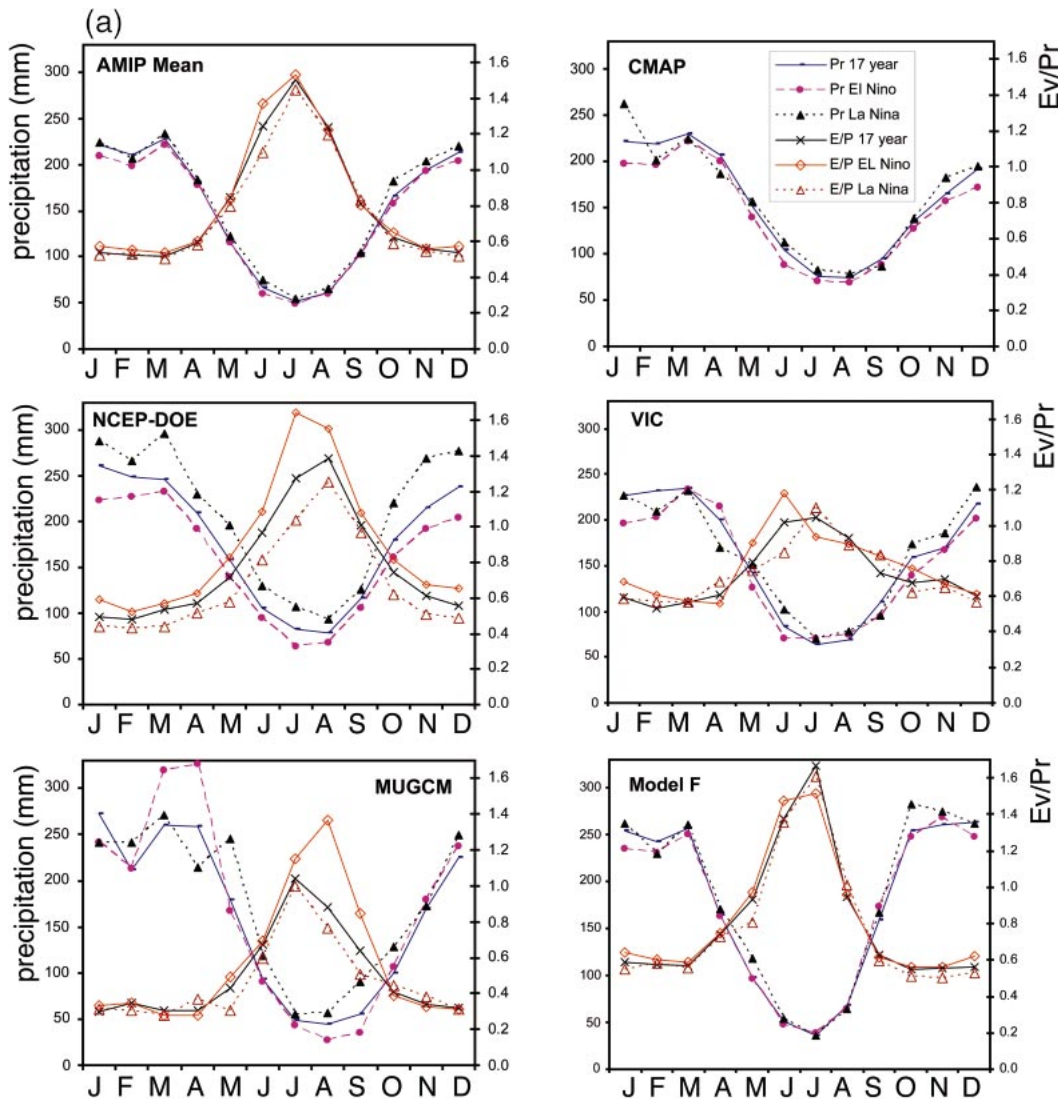


FIG. 4. Seasonal cycles of precipitation (Pr; left scale) and evaporation ratio (Ev/Pr; right scale) for the three basins: (a) Amazon, (b) Murray–Darling, and (c) Mississippi. The observations of precipitation (top right; CMAP) are compared with model predictions from the mean of 20 AMIP II models; the NCEP–DOE reanalysis; VIC; MUGCM; and AMIP II model F. Also shown are the excursions caused by the El Niños and La Niñas that occurred during the 17-yr AMIP II simulation period. [The point off-scale for MUGCM in (b) is 5.1.]

torily in the three basins of interest here. The large variations among the representations of the evaporation ratio suggest that the subtleties of precipitation partition, precisely where isotopic characteristics are hoped to add benefit, are likely to be differently characterized by these models. This result is similar to the conclusion drawn regarding the partition of net surface energy (see Fig. 3).

The two models examined have basin-scale water budget characteristics similar to many others in use currently. The veracity of their simulations, while not being implausible, cannot be verified with available observations. While some aspects of these simulations may render surface water characterization questionable, the

MUGCM and AMIP II model F are no worse than similar models. The hypothesis we pursue here is that aspects of the gross water fluxes may be explained and improved by isotopic investigation.

3. Evaluating stable water isotope simulations

Deviations from the MWL are usually expressed in terms of the “deuterium excess” parameter defined as $d = \delta D - 8\delta^{18}O$ (Dansgaard 1964) (Fig. 1). Departures from a value of 10 for the deuterium excess indicate a secondary source of either isotopically depleted or enriched water vapor (Gat and Matsui 1991). Using Global Network for Isotopes in Precipitation (GNIP) data,

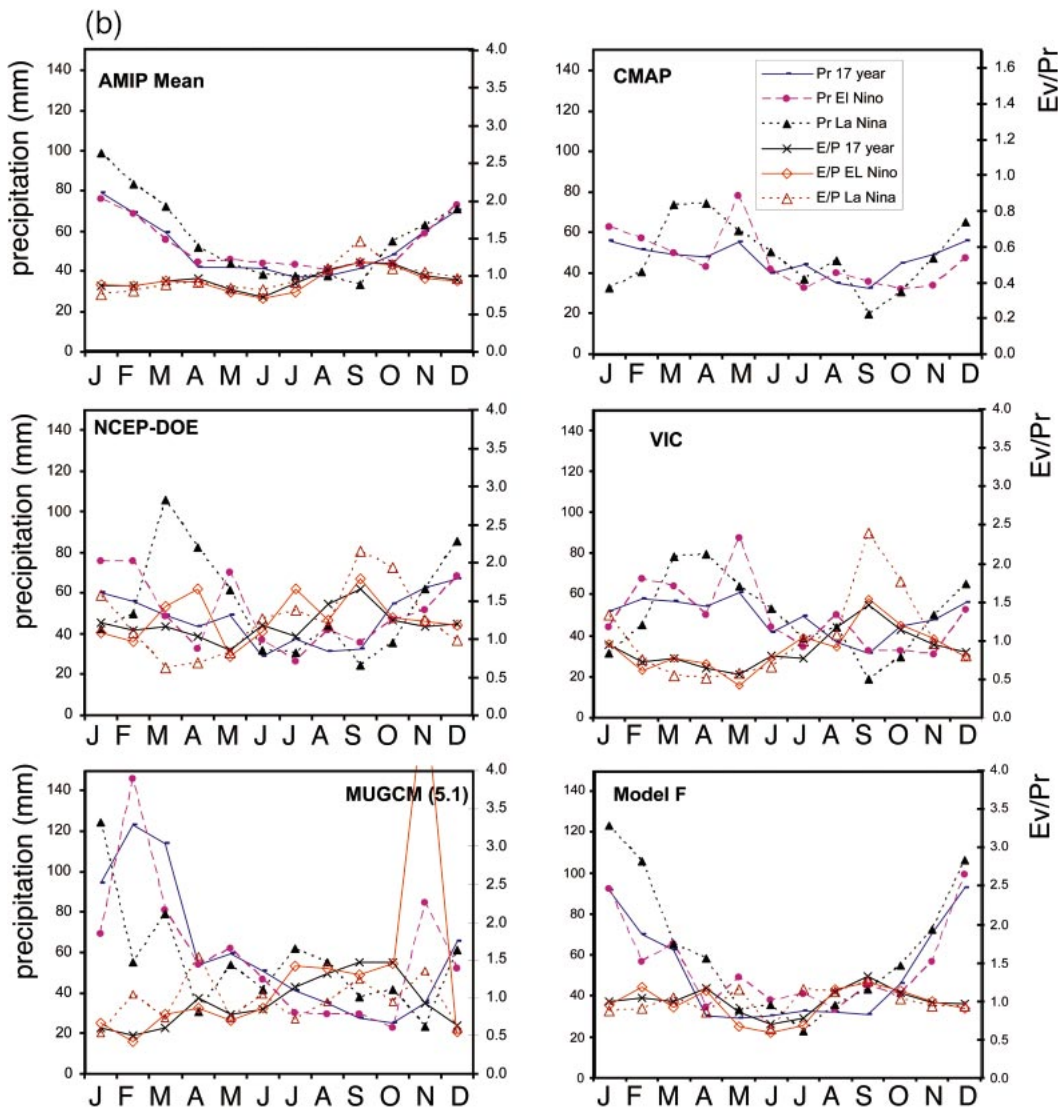


FIG. 4. (Continued)

Froehlich et al. (2002) find that an increase of the deuterium excess of about 5‰ corresponds with a recycling ratio from open water surfaces of about 5%, for the Great Lakes region in good agreement with the earlier evaluation by Gat et al. (1994). They also find *d*-excess values in the range of +20‰, indicating a recycling ratio close to 20%.

a. Precipitation isotopes from GNIP and the MUGCM

Two precipitation measures of $\delta^{18}\text{O}$ and δD are examined here. The first of these is taken from GNIP observations (IAEA 2001) (Table 2) and the second from the MUGCM (Noone and Simmonds 2002). The GNIP reports of both $\delta^{18}\text{O}$ and δD range in quality and quantity in the three basins: the Mississippi having few

stations (many reporting only tritium), the Amazon very many, and the Murray–Darling strictly only one. Here we have tried to select two representative GNIP stations in each basin (Chicago and Waco in the Mississippi; Manaus and Izobamba in the Amazon, and Brisbane and Adelaide in the Murray–Darling), and from these we use the mean monthly values of $\delta^{18}\text{O}$ and δD recorded in, and weighted by, precipitation. Table 2a gives the length of the available data record and the precipitation-weighted averages and standard deviations (std devs) for $\delta^{18}\text{O}$ and δD from these six stations. It is clear that the significant differences between these basin pairs would render averages among them unhelpful and, since only one or two stations exist, basinwide averages are impossible. Instead we have identified a preferred station in each basin (Chicago, Manaus, and Brisbane) and list their monthly

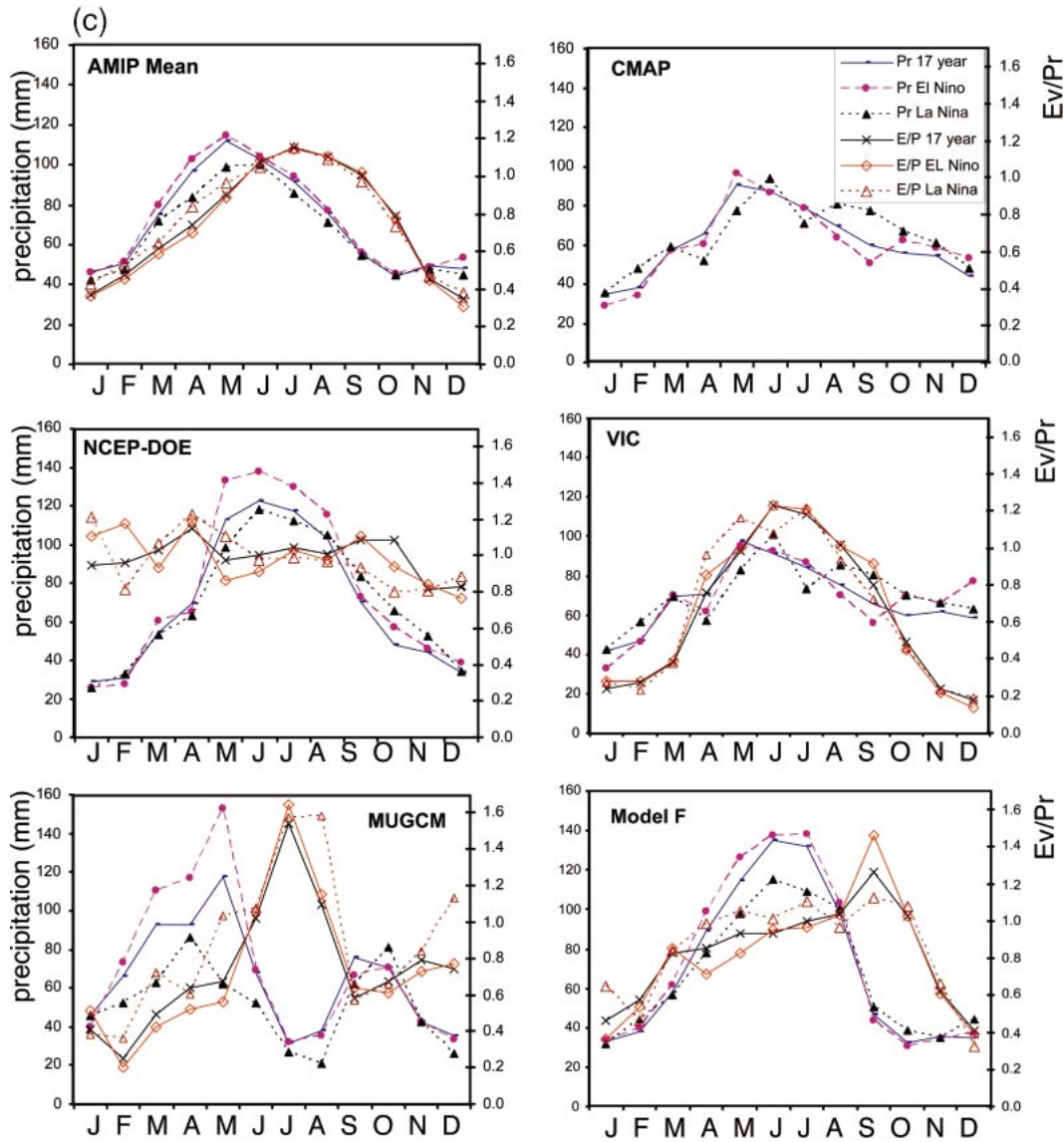


FIG. 4. (Continued)

TABLE 2a. Station names and numbers of years for pairs of GNIP stations in each basin's isotope record together with precipitation-weighted $\delta^{18}\text{O}$ and δD .

| Station (basin) | Location | Altitude (m MSL) | Years in GNIP reports | No. of months | Both D and ^{18}O | $\delta^{18}\text{O}$ and δD (and std devs) (‰) |
|---------------------------|-------------------|------------------|-----------------------|---------------|----------------------------|---|
| Manaus (Amazon) | 3.12°S, 60.02°W | 7 | 1965–90 | 201 | 78% | -5.13 (2.7), -28.52 (22.2) |
| Izobamba (Amazon) | 0.37°S, 78.55°W | 3058 | 1968–2000 | 254 | 76% | -10.76 (3.6), -74.95 (29.0) |
| Chicago (Mississippi) | 41.78°N, 87.75°W | 189 | 1962–79 | 213 | 79% | -6.48 (4.8), -44.31 (34.5) |
| Waco (Mississippi) | 31.62°N, 97.22°W | 156 | 1961–86 | 268 | 35% | -4.04 (2.7), -22.87 (18.2) |
| Brisbane (Murray–Darling) | 27.43°S, 153.08°E | 4 | 1962–2000 | 414 | 76% | -4.19 (2.1), -20.24 (16.7) |
| Adelaide (Murray–Darling) | 34.93°S, 138.58°E | 43 | 1962–86 | 199 | 56% | -4.50 (2.4), -24.57 (18.4) |

means and standard deviations of $\delta^{18}\text{O}$ and δD in Table 2b.

Figure 5 shows the seasonal cycle in $\delta^{18}\text{O}$ and deuterium excess in precipitation from observations (GNIP) and from the MUGCM. The error bars on the observations are of ± 1 standard error (SE) over the total length of the GNIP record [which differs across the three basins (Table 2a)]. For $\delta^{18}\text{O}$, the seasonal cycle and absolute values in all three basins are fairly well represented by the MUGCM. In the Murray–Darling basin, values and seasonality are least successful, lying outside both the two stations and their error bars for 5 of the 12 months. Specifically, values tend to be too low (overly depleted), and the seasonal cycle is larger than and different to (least depleted around September) the observed. In the Amazon and the Murray–Darling, the model underestimates d excess by about 2‰–3‰ but overestimates it in the Mississippi. The poor seasonality can be traced back to relatively poor total precipitation prediction by MUGCM in this basin. The MUGCM deuterium excess values are similar in the three basins and throughout the year. The lack of seasonality arises because the $\delta^{18}\text{O}$ and δD values in the MUGCM precipitation track one another more closely than is observed. The much flatter prediction of d excess in the Mississippi than observed in GNIP suggests that the MUGCM is not fully capturing the seasonal variations in moisture sources. This may indicate that the simulation of the origin and intensity of major rain- and snow-bearing storms in this region warrant investigation.

Figure 5 and Table 3 show that the isotopic precipitation characteristics of the MUGCM differ from observations. Specifically, $\delta^{18}\text{O}$ and δD are quite close to the observed annual mean in the Mississippi; approximately 50% too depleted in the Murray–Darling; and roughly double the observed depletions in the Amazon. The seasonal range in $\delta^{18}\text{O}$ and δD are close to observed in the Amazon and the Murray–Darling but only about one-quarter of the observed in the Mississippi. This similar behavior for different basins is likely to be related

to the overall abundances of the isotopes in the global atmosphere. For example, the MUGCM underestimates d excess by $\sim 2\%$ globally as a result of surface exchange parameterization over the ocean and overly simple simulation of cloud processes.

The seasonality in the Amazon is modeled reasonably well although it suffers from an annual offset of a few percent. The summer precipitation is low, probably because the intense and high precipitation rate convection season (or monsoon) is rather weak in the MUGCM (Fig. 5); that is, the problems in the seasonality are indicative of the shortcoming of the global- to regional-scale sources of catchment moisture. While MUGCM is predicting the precipitation seasonality with fidelity, we conclude from the isotopic analysis that the specific combination of processes governing the seasonal precipitation is not correctly captured by this model.

Annually averaged deuterium excess values from the MUGCM are listed in Table 3. Froehlich et al. (2002) propose that the deuterium excess can be used as a fingerprint of the oceanic source area of the precipitation collected at a given station and also as characterizing mixing of air during passage to the point of precipitation data collection. Because $\delta^{18}\text{O}$ and δD are, for the most part, similar under equilibrium conditions, the relationship between them is very sensitive to exposure to non-equilibrium environments. Examples include surface evaporation and evaporation of falling precipitation into very dry continental air. As such, the d excess captures different aspects of the conditions of moisture transport, mixing, and condensation than the abundance of a single isotope. Simulated transects of d excess might provide insight into the continental effect as atmospheric moisture evolves by progressive rainout and mixing processes over the continents (e.g., Gonfiantini et al. 2001) or merely the poor parameterization of these effects. Values of d excess in Table 3 and Fig. 5 suggest that some aspects of the MUGCM basin-scale simulations lack credibility. The use of the d -excess parameter as a

TABLE 2b. Observed precipitation-weighted $\delta^{18}\text{O}$ and δD for the three basins derived from the preferred GNIP station for all of the available record giving means and std devs.

| GNIP Month | Mississippi (Chicago) | | Murray–Darling (Brisbane) | | Amazon (Manaus) | |
|---------------|---|--|---|--------------------------------|---|--|
| | Mean (std dev) $\delta^{18}\text{O}$ (‰) | Mean (std dev) δD (‰) | Mean (std dev) $\delta^{18}\text{O}$ (‰) | Mean (std dev) δ (‰) | Mean (std dev) $\delta^{18}\text{O}$ (‰) | Mean (std dev) δD (‰) |
| Jan | −14.02 (4.90) | −98.87 (37.6) | −4.61 (1.81) | −25.55 (15.5) | −4.24 (1.41) | −21.68 (11.3) |
| Feb | −12.17 (3.52) | −87.41 (24.6) | −3.26 (1.61) | −16.05 (13.0) | −5.13 (1.92) | −28.61 (15.9) |
| Mar | −7.92 (3.33) | −54.47 (28.0) | −4.48 (2.07) | −25.00 (16.1) | −6.87 (2.54) | −43.14 (20.0) |
| Apr | −6.11 (2.39) | −40.17 (17.0) | −4.54 (2.15) | −22.29 (17.2) | −7.19 (2.28) | −45.30 (20.4) |
| May | −5.21 (3.43) | −37.87 (22.1) | −5.73 (2.32) | −31.45 (19.6) | −7.89 (3.64) | −45.09 (30.5) |
| Jun | −3.15 (3.18) | −24.09 (22.0) | −4.59 (1.69) | −20.70 (13.5) | −4.10 (2.13) | −18.98 (17.8) |
| Jul | −3.25 (1.81) | −19.36 (8.3) | −6.58 (3.19) | −36.81 (26.4) | −3.3 (1.52) | −10.11 (14.0) |
| Aug | −4.15 (2.24) | −28.11 (12.9) | −3.50 (1.47) | −12.00 (12.9) | −1.97 (1.75) | −1.47 (15.7) |
| Sep | −5.11 (2.57) | −36.60 (12.1) | −3.11 (1.98) | −4.15 (15.6) | −2.00 (1.44) | −2.59 (9.2) |
| Oct | −6.14 (2.94) | −40.75 (21.4) | −2.69 (1.44) | −7.27 (12.3) | −2.35 (1.25) | −5.35 (8.9) |
| Nov | −8.81 (4.20) | −58.61 (32.1) | −3.15 (2.00) | −11.84 (13.8) | −3.81 (2.25) | −17.81 (16.3) |
| Dec | −11.30 (3.54) | −74.46 (30.5) | −3.63 (1.52) | −15.25 (13.4) | −3.44 (1.23) | −16.61 (8.2) |

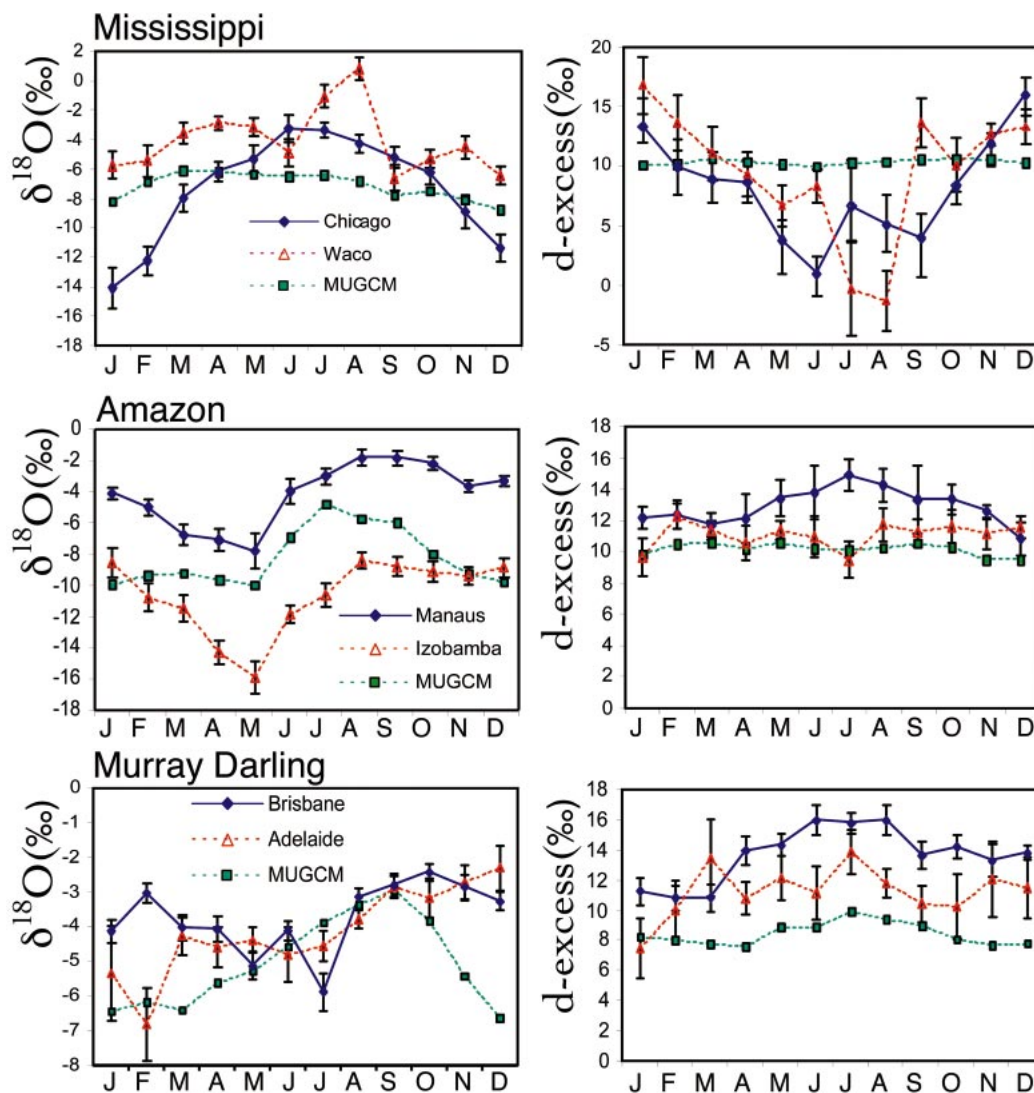


FIG. 5. Seasonal cycles of precipitation-weighted $\delta^{18}\text{O}$ and deuterium (d) excess in precipitation for the three basins (the Mississippi: Chicago and Waco; the Amazon: Manaus and Izobamba; and the Murray–Darling: Brisbane and Adelaide) from GNIP observations and MUGCM. Error bars are ± 1 SE are shown on the GNIP data. All available data are used in all cases (see Table 2a).

TABLE 3. Comparison of basin precipitation-weighted isotopic statistics from the preferred GNIP station (see Table 2a) and the MUGCM.

| Isotopic characteristic | Annual mean $\delta^{18}\text{O}$ (‰) | Monthly mean range $\delta^{18}\text{O}$ (‰) | Annual mean δD (‰) | Monthly mean range δD (‰) | Slope δD against $\delta^{18}\text{O}$ | Deuterium excess (d) (‰) |
|-------------------------|---------------------------------------|--|----------------------------------|---|--|------------------------------|
| Murray–Darling | | | | | | |
| Brisbane GNIP | −4.19 | 3.89 | −20.24 | 29.54 | 7.71 | 13.31 |
| MUGCM | −5.64 | 4.15 | −36.61 | 34.41 | 8.37 | 8.49 |
| Amazon | | | | | | |
| Manaus GNIP | −5.13 | 5.91 | −28.52 | 48.17 | 8.14 | 12.22 |
| MUGCM | −8.28 | 5.12 | −56.08 | 41.07 | 8.08 | 10.15 |
| Mississippi | | | | | | |
| Chicago GNIP | −6.48 | 10.87 | −44.31 | 79.50 | 7.00 | 7.53 |
| MUGCM | −7.03 | 2.74 | −45.90 | 22.30 | 7.98 | 10.37 |

probe of such shortcomings is examined in the next section.

The seasonality and absolute values of both $\delta^{18}\text{O}$ and δD predicted by the MUGCM are found to be less than satisfactory in the Mississippi; open to investigation and improvement in the Amazon; and difficult to assess in the Murray–Darling because of the highly variable precipitation, which depend upon both $\delta^{18}\text{O}$ and δD , are challenging to interpret with respect to basin-scale surface water budgets. However, these d -excess values do seem to have the potential to be powerful diagnostics of complex effects involving interactions between local evaporation and large-scale moisture budgets. For example, in the Mississippi, the lack of seasonality in d excess suggests poor simulation of the origin and intensity of major storms in this region by the MUGCM [cf. Froehlich et al. (2002) who find an increase of d excess of up to 5‰ near the Great Lakes]. It may also reflect failure of the AGCM, which has a rather coarse resolution, to capture the lake isotopic effects important in the eastern part of the Mississippi and, arguably, open water and foliage effects in the Amazon.

b. Isotopic enrichment in the surface water system from ISOLSM

ISOLSM computes the isotopic enrichment (or depletion) of surface water fluxes and reservoirs given an imposed isotopic concentration in precipitation and near-surface atmospheric vapor (Riley et al. 2002). Here, we force ISOLSM with NCEP reanalysis meteorology every 6 h and prescribe the isotopic ratios of precipitation and atmospheric water vapor as equivalent to the Vienna Standard Mean Ocean Water (V-SMOW) standard. The precipitation is the principal input to the land scheme, while atmospheric vapor controls the water loss by evaporation and transpiration. By setting the isotopic condition of these waters we can evaluate the consequence of terrestrial exchanges as deviations from SMOW. In particular, we analyse the terrestrial results relative to (as a difference from) the precipitation ($\delta = 0$) and evaluate the success with which these major controls on the variability of ^{18}O and deuterium are captured by our two example models. We do this by examining the ^{18}O and D characteristics of a variety of water pools in the three large river basins: the Amazon, the Murray–Darling, and the Mississippi.

Prescribing the same isotopic ratio for both precipitation and atmospheric water vapor is rather unrealistic since ambient air water vapor is more likely to be in near equilibrium with precipitation (if unfrozen). The motivation is that such prescription allows control of the model response in the absence of measurements with which to force the model, but it has implications for interpretation of the results.

Figure 6 shows the delta distributions of $\delta^{18}\text{O}$ against δD for the three basins for evaporative leaf water (water

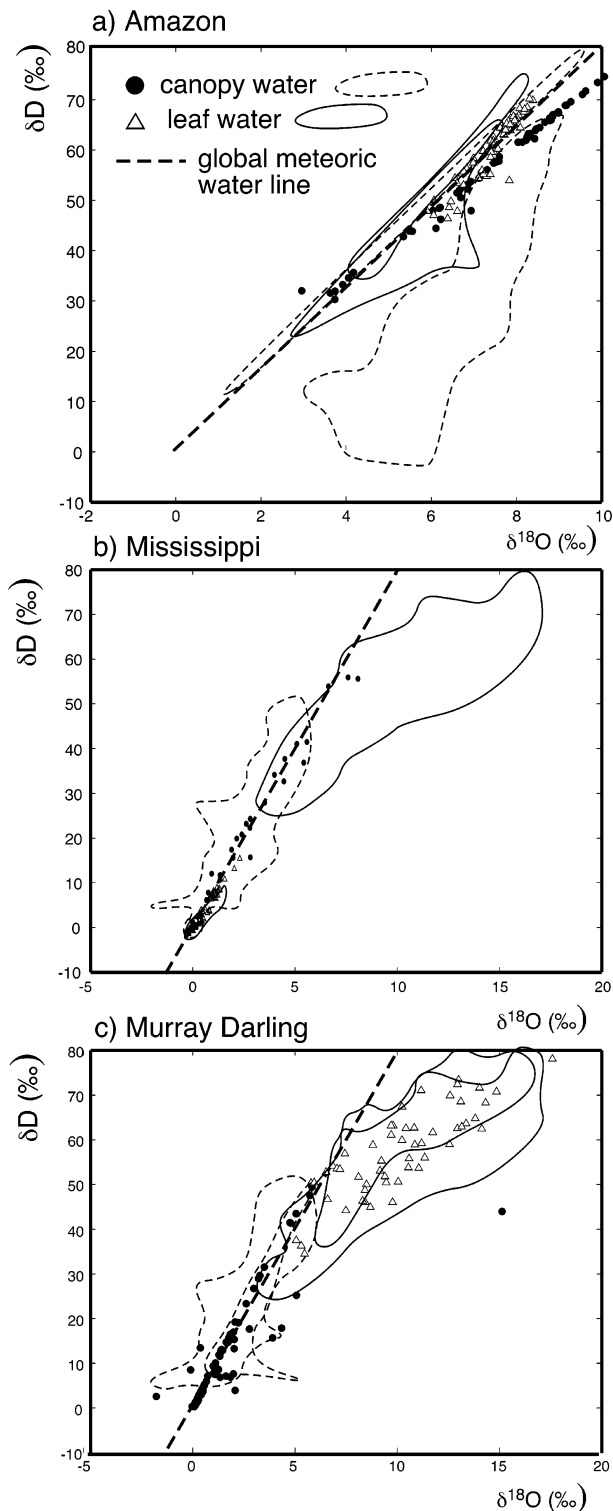


FIG. 6. Simulations in (a) the Amazon, (b) the Mississippi, and (c) the Murray–Darling by ISOLSM of stable water isotopic ($\delta^{18}\text{O}$ and δD) offsets from V-SMOW for intercepted canopy water and leaf surface evaporative water at two randomly selected points (solid circles for canopy water and open triangles for leaf water) and the basin averages for every month in a 5-yr offline simulation (envelopes: dashed for canopy water and solid for leaf water). All values are enrichments relative to the precipitation (prescribed as V-SMOW).

inside the leaf stomates) and canopy-intercepted water (precipitated water caught on foliage). The enrichment in heavy water isotopes is clearly seen in these two components. One notable feature is the different relative gradients for leaf water and canopy-intercepted moisture between the Amazon and the Murray–Darling. This may be due to the different moisture availability in the two basins and the resulting stresses on plant behavior. Since in this simulation the canopy humidity is prescribed (NCEP forcing), there is no feedback to the atmosphere from evaporation processes, which may also be contributing to these unusual results. In addition, the two canopy reservoirs also show a near-linear relationship in the Amazon with slopes close to that of the global MWL. In the Murray–Darling and the Mississippi, however, the relationships are not linear (low correlations) and the best-fit slopes are very much less than the forcing precipitation and soil components.

Departure from the slope of the MWL in Fig. 6 indicates the importance of nonequilibrium processes in the evaporation. In the Amazon, these may also be the result of the more extensive canopy reservoir and/or greater turnover of reservoirs. Neither land surface scheme includes (in the implementations used here) the explicit effect of open water. As a consequence, river water and soil water reflect closely the isotopic characteristics of the precipitation (cf. Fig. 8), a departure from observed, where lake and river evaporation play a role in determining the isotopic enrichment of these reservoirs.

If the ISOLSM simulations of the isotopic enrichment persisted in coupled atmosphere–land models, they would result in larger changes for canopy water components, with the Amazon exhibiting a different distribution from the other two basins. The very similar isotopic enrichment in the leaf water and the canopy-intercepted rainfall in the Amazon is particularly surprising.

Although there is a good global distribution of measurements of stable water isotopes in precipitation, available data on river water and, particularly, plant water and vapor are much sparser. Figure 7 illustrates the types of observations becoming available through the new IAEA Global Network for Isotopes in Rivers (GNIR; Gibson et al. 2002). Figure 7a shows $\delta^{18}\text{O}$ values for the Amazon forest plants while Fig. 7b illustrates isotopic characteristics for the Darling River (the upper part of the Murray–Darling basin) for the period July 2002 to January 2003. The range of $\delta^{18}\text{O}$ values in Fig. 7a (0‰ to -4 ‰ for sap water and 0‰ to $+10$ ‰ for leaf water) are in good agreement with the calculated offset values from ISOLSM for foliage water if these are added to representative precipitation values for $\delta^{18}\text{O}$ (Table 2 and Fig. 5). In the Mississippi (Fig. 6b), the basin-mean evaporative leaf water has $\delta^{18}\text{O}$ offsets ranging from ~ -0.5 ‰ to $+3$ ‰ while the canopy-intercepted water offsets are from $\sim +1$ ‰ to $+8$ ‰. These values compare adequately with Riley et al.'s (2003)

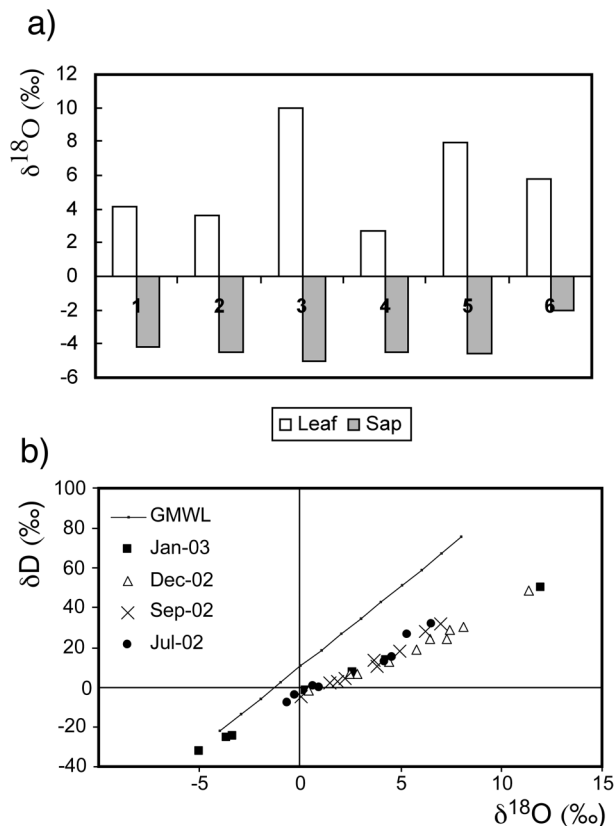


FIG. 7. Selected isotopic observations from the Murray–Darling and Amazon basins for surface water budget components other than precipitation: (a) $\delta^{18}\text{O}$ values of bulk leaf water and sap water of plants collected in the shore of the Lake Grande in Sep 2002 (after Martinelli 2003), and (b) $\delta^{18}\text{O}$ versus δD relationship from the Darling River for the period Jul 2002 to Jan 2003 (after Stone et al. 2003).

reports of leaf water $\delta^{18}\text{O}$ observations of $+7$ ‰ to $+15$ ‰ and stem water values between 0 ‰ and -5 ‰ from a tallgrass prairie in the central Mississippi basin.

Figure 7b is more difficult to compare with the foliage offset values in Fig. 6. Canopy-intercepted water might be considered to be weakly related to the drought-stressed Darling River water because both are evaporatively enriched. The ISOLSM offsets for canopy water range from 0 ‰ to $+6$ ‰ for $\delta^{18}\text{O}$ and from 0 ‰ to $+50$ ‰ for δD giving some agreement with the central group of observations in Fig. 7b when added to appropriate precipitation values (Table 2). Figure 8 shows time series of the deuterium excess at two grid points in each basin of four ISOLSM variables now including overland flow and soil drainage. The Fig. 7b values of d range between 10 ‰ and 20 ‰ comparable to those of leaf evaporative water but not with either of the soil water parameters that have precipitation-like d excesses.

The most interesting feature is the differences in behavior between the Amazon and the other two basins: Amazonian leaf water exhibits significant enrichment in δD : the values lie above the MWL. In the Mississippi and Murray–Darling, evaporative surface leaf water, al-

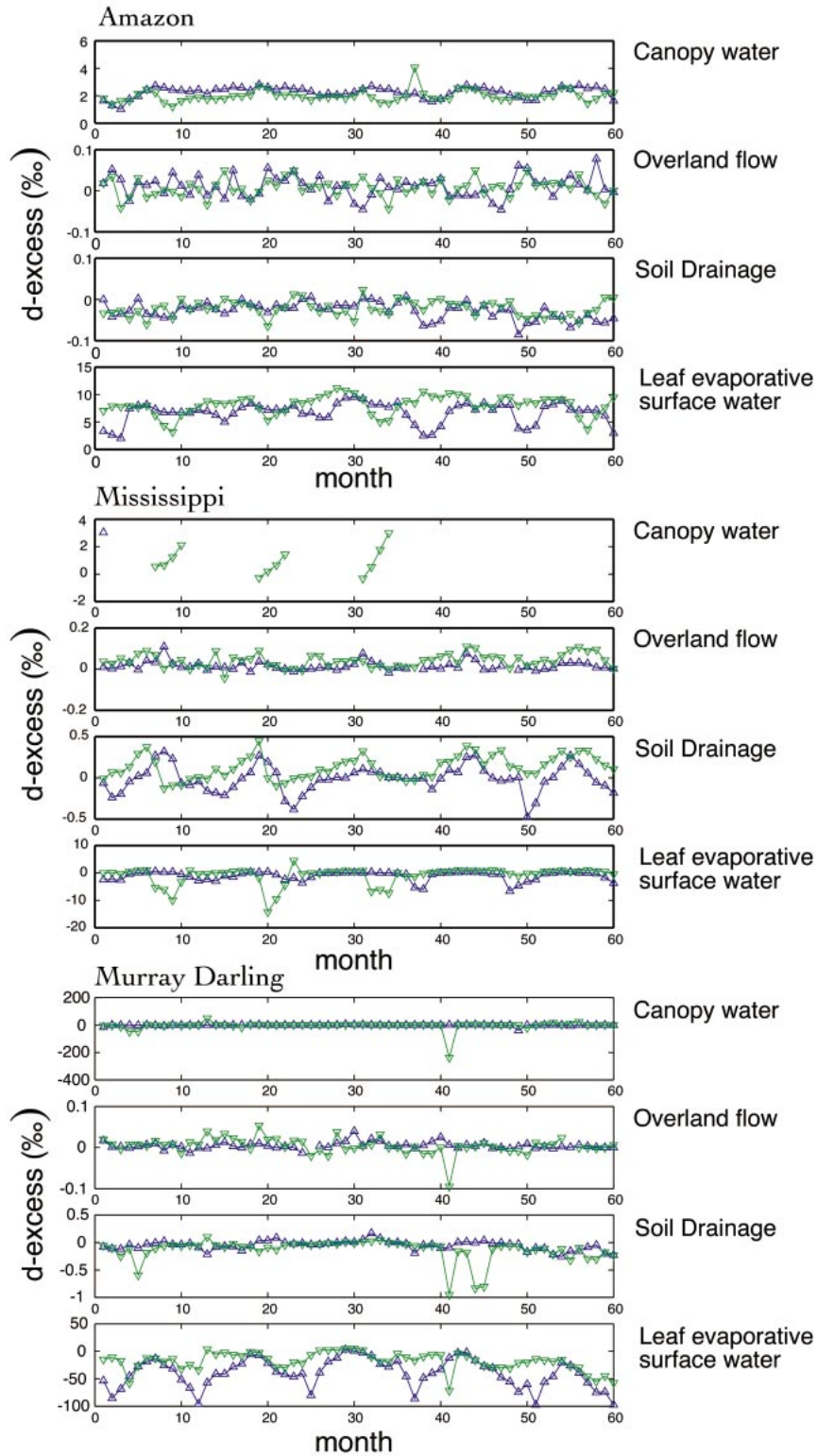


FIG. 8. Deuterium excess offsets from ISOLSM for 5 yr of offline integration for two randomly selected "points" in each of the three basins: (top) Amazon, (middle) Mississippi, and (bottom) Murray-Darling. Four surface water variables are shown: intercepted canopy water, soil surface runoff (overland flow), deep soil drainage, and leaf surface evaporative water.

though isotopically enriched compared to all other components (values of $\delta^{18}\text{O}$ and δD are larger than, e.g., runoff) the lower δD values suggest nonequilibrium processes as expected with evaporation into unsaturated vapor. In addition, the values of $\delta^{18}\text{O}$ in leaf and canopy-intercepted water are larger than in the Amazon. This may be because the larger rainfall amounts in the Amazon cause a faster replacement by washoff of existing water from the canopy reservoir, resulting in a lesser enrichment of the canopy water. In the Mississippi and the Murray–Darling, the precipitation stays longer on the canopy and is enriched more by evaporative processes. Overall, ISOLSM is able to calculate plausible values of $\delta^{18}\text{O}$ and δD in terms of depletions/enrichments relative to precipitation (e.g., Table 2). Validation data are available only at point locations, but are in broad agreement with the numerical simulations.

c. Sensitivity in prediction of isotopic characteristics

For numerical simulations of stable water isotopes to be correct and useful in climate and earth system models, the “big leaf” assumptions underpinning current land surface parameterizations must be properly implemented and must “scale” for water isotopes at least as well as for gross (i.e., total) water fluxes. To investigate this we have considered two grid points in each basin. Figure 6 also shows the offset δ values computed in ISOLSM for leaf water and canopy-intercepted water for two separate grid points (as envelopes), and Figure 8 represents just the data from these two points.

The large dispersion, especially of the envelopes in Fig. 6, underlines the work required in the analysis of spatial variability and the basin-scale integration of isotopic characteristics because of their dependence upon (poorly resolved) small-scale processes. Specifically, at present there is a lack of data sufficient to assess simulation of isotopic state of terrestrial waters at anything beyond specially instrumented sites. While such observations are invaluable to examine processes modeled, the applicability to upscaling to basin and continental scales cannot be addressed. In particular, there are, at present, no global, or even basinwide, observations of the ^{18}O and D in near-surface atmospheric vapor, which is needed to close the surface exchange calculations. Similarly, large-scale measurements of leaf, stem, and soil water do not exist, against which the present simulations would most naturally be compared.

Additionally, the time scales of motion of water through the various reservoirs must be explored. The annual cycles are clear in Fig. 8: most pronounced in the Murray–Darling basin. The 6-month periodicity in the Amazon results for evaporative leaf surface water is a result of the intertropical convergence zone (ITCZ) cycle in precipitation. This dependence on moisture rather than temperature is explicable since, while the amount of fractionation for each individual isotope is determined by the degree of distillation the air mass

undergoes during transport, the d value reflects non-equilibrium fractionation during initial evaporation from the oceans, reevaporation at the land surface, or reevaporation along the air mass’s trajectory (Merlivat and Jouzel 1979).

4. Stable water isotopes in basin-scale simulations

Isotopes of water have been simulated in global models since the 1980s (e.g., Jouzel et al. 1987, 1991) and exploited in observational interpretation since well before this (e.g., Dansgaard, 1964; Gat 2000). These isotopes exhibit power in diagnosing limitations in components of numerical models at the basin scale in applications in which observed isotopic histories are compared with simulations (Henderson-Sellers et al. 2002; Hoffman et al. 2003).

Aspects of the simulation of stable water isotopic behavior have been investigated here in order to evaluate the utility of reconciling known shortcomings in global climate or earth system models that arise from mismatch between spatial scales under consideration (i.e., coarse-resolution basin-scale surface water budgets and fluxes versus more detailed exchange processes). We find that the MUGCM global- and basin-scale precipitation relationships between $\delta^{18}\text{O}$ and δD (gradient around 8) and between $\delta^{18}\text{O}$ and temperature are broadly satisfactory, and that LSM (employed as the basis for ISOLSM) closes its water balance and predicts plausible budgets in a coupled mode. While many of the processes necessary for appropriate simulation of isotopic fluxes in basin-scale hydrology can be demonstrated, the “big leaf” representation of land surfaces in climate models does not necessarily provide adequate mechanistic characterization for water isotopes. Specifically, the integration up to the basin scale of a large number of local flux components, each of which may have locally differing isotopic signatures in nature, makes it difficult to make quantitative isotopic assessments of water and energy flux estimates derived from a single “big leaf” scheme.

The roles of deep soil water and groundwater as storage reservoirs and hence sources for delayed evaporative and streamflow fluxes have been investigated in land surface intercomparisons (e.g., Yang et al. 1995). Isotopic differentiation between precipitation, groundwater, and river runoff may offer a novel means of establishing the time scales of storages and relative flushing rates (e.g., Gibson et al. 2002; Airey et al. 2003).

At present we must conclude that surface water budgets are still rather poorly simulated and badly constrained at the scale of large basins, and surface energy partition can be apparently well captured by models with inadequate land surface parameterization and fluxes. As such, budgets of the isotopes H_2^{18}O and $^1\text{H}^2\text{H}^{16}\text{O}$ are not yet able to be simulated adequately, which provides both renewed motivation and additional constraints for improving surface exchange schemes. While HDO and

$H_2^{18}O$ simulations are substantially influenced by current inadequacies in basin-scale hydrological simulation, their strength is in elucidating aspects of these shortcomings in the underlying models. We have been able here to deduce information from isotopes that would otherwise have been undetectable. In particular, for the two models examined in detail, isotopic interpretations have shown the energy balance is correct for the wrong reasons (i.e., isotopes show water budgets are incorrect) and that the net convergence and recycling of water in the atmosphere can be deduced from stable isotopes of water and leads to additional information about the gross water fluxes. However, a much more comprehensive set of observations and integrative simulations are needed to make conclusive statements on the accuracy of hydrologic simulations from climate system models on global and even basin scales.

Acknowledgments. This work was conducted while AH-S and KMcG were visitors at the National Snow and Ice Data Center (NSIDC) in Boulder, the former as a University of Colorado CIRES Visiting Fellow. L. Dyer retrieved some of the AMIP and MUGCM results. We appreciate useful input from three anonymous reviewers.

REFERENCES

- Airey, P., A. Henderson-Sellers, M. A. Habermehl, J. Bradd, S. Chambers, and C. Hughes, 2003: Sustainability of groundwater under climate change. *Proc. IAEA Symp. on Isotope Hydrology and Integrated Water Resources Management*, Vienna, Austria, IAEA, IAEA CN-104/P16, 140–141.
- Berg, A. A., J. S. Famiglietti, J. P. Walker, and P. R. Houser, 2003: Impact of bias correction to reanalysis products on simulations of North American soil moisture and hydrological fluxes. *J. Geophys. Res.*, **108**, 4490, doi:10.1029/2002JD003334.
- Craig, H., 1961: Isotopic variations in meteoric water. *Science*, **133**, 1702–1703.
- Dansgaard, W., 1964: Stable isotopes in precipitation. *Tellus*, **16**, 436–468.
- Fekete, B. M., C. J. Vorosmarty, and W. Grabs, 2000: Global, composite runoff fields based on observed river discharge and simulated water balances. GRDC Rep. 22, 36 pp. [Available online at www.grdc.sr.unh.edu/html/Data/runoff.zip.]
- Froehlich, K., J. J. Gibson, and P. Aggarwal, 2002: Deuterium excess in precipitation and its climatological significance. *Proc. Int. Conf. on Study of Environmental Change Using Isotope Techniques*, C&S Papers Series 13/P, Vienna, Austria, International Atomic Energy Agency, 54–66.
- Gat, J. R., 1996: Oxygen and hydrogen isotopes in the hydrological cycle. *Annu. Rev. Earth Planet. Sci.*, **24**, 225–262.
- , 2000: Atmospheric water balance—The isotopic perspective. *Hydrol. Processes*, **14**, 1357–1369.
- , and E. Matsui, 1991: Atmospheric water balance in the Amazon basin: An isotopic evapotranspiration model. *J. Geophys. Res.*, **96** (D7), 13 179–13 188.
- , C. J. Browser, and C. Kendall, 1994: The contribution of evaporation from the Great Lakes to the continental atmosphere: Estimate based on stable isotope data. *Geophys. Res. Lett.*, **21**, 557–560.
- Gates, W. L., 1992: The atmospheric model intercomparison project. *Bull. Amer. Meteor. Soc.*, **73**, 1962–1970.
- , and Coauthors, 1999: An overview of the results of the Atmospheric Model Intercomparison Project (AMIP I). *Bull. Amer. Meteor. Soc.*, **80**, 29–55.
- Gibson, J. J., 2002: Short-term evaporation and water budget comparisons in shallow Arctic lakes using non-steady isotope mass balance. *J. Hydrol.*, **264**, 242–261.
- , and T. W. D. Edwards, 2002: Regional water balance trends and evaporation–transpiration partitioning from a stable isotope survey of lakes in northern Canada. *Global Biogeochem. Cycles*, **16**, 1026, doi:10.1029/2001GB001839.
- , and Coauthors, 2002: Isotope studies in large river basins: A new global research focus. *Eos, Trans. Amer. Geophys. Union*, **83**, 613–617.
- Gibson, J. K., P. Kallberg, S. Uppala, A. Hernandez, A. Normura, and E. Serrano, 1997: ERA description. ECMWF Re-Analysis Project Report Series 1, 72 pp.
- Gonfiantini, R., M. A. Roche, J. C. Olivry, and G. M. Zuppi, 2001: The altitude effect on isotopic composition of tropical rains. *Chem. Geol.*, **181**, 147–167.
- Henderson-Sellers, A., A. J. Pitman, P. K. Love, P. Irannejad, and T. H. Chen, 1995: The Project for Intercomparison of Land surface Parameterization Schemes (PILPS): Phases 2 and 3. *Bull. Amer. Meteor. Soc.*, **76**, 1962–1970.
- , K. McGuffie, and H. Zhang, 2002: Stable isotopes as validation tools for global climate model predictions of the impact of Amazonian deforestation. *J. Climate*, **15**, 2664–2677.
- , P. Irannejad, K. McGuffie, and A. J. Pitman, 2003a: Predicting land-surface climates—Better skill or moving targets? *Geophys. Res. Lett.*, **30**, 1777, doi:10.1029/2003GL017387.
- , —, —, S. Sharmeen, T. J. Phillips, K. McGuffie, and H. Zhang, 2003b: Evaluating GEWEX CSEs' simulated land-surface water budget components. *GEWEX News*, Vol. 13, No. 3, International GEWEX Project Office, Silver Spring, MD, 3–6.
- Hoffman, G., and Coauthors, 2003: Coherent isotope history of Andean ice cores over the last century. *Geophys. Res. Lett.*, **30**, 1179, doi:10.1029/2002GL014870.
- Houghton, J. T., Y. Ding, D. J. Griggs, M. Noguer, P. J. van der Linden, X. Dai, K. Maskell, and C. A. Johnson, Eds., 2001: *Climate Change 2001: The Scientific Basis*. Cambridge University Press, 881 pp.
- IAEA, cited 2001: Isotope Hydrology Information System: The ISOHIS Database. [Available online at <http://isohis.iaea.org>.]
- Ingraham, N. L., and R. C. Craig, 1986: Hydrogen isotope study of large-scale meteoric water transport in northern California and Nevada. *J. Hydrol.*, **85**, 183–197.
- Irannejad, P., A. Henderson-Sellers, and S. Sharmeen, 2003: Importance of land-surface parameterization for latent heat simulation in global atmospheric models. *Geophys. Res. Lett.*, **30**, 1904, doi:10.1029/2003GL018044.
- Joussaume, S., and J. Jouzel, 1993: Paleoclimatic tracers: An investigation using an atmospheric general circulation model under ice age conditions. 2. Water isotopes. *J. Geophys. Res.*, **98**, 2807–2830.
- , R. Sadourny, and J. Jouzel, 1984: A general circulation model of water isotopes cycles in the atmosphere. *Nature*, **311**, 24–29.
- Jouzel, J., G. L. Russell, R. J. Suozzo, R. D. Koster, J. W. C. White, and W. S. Broecker, 1987: Simulations of the HDO and $H_2^{18}O$ atmospheric cycles using the NASA GISS General Circulation Model: The seasonal cycle for present day conditions. *J. Geophys. Res.*, **92**, 14 739–14 760.
- , R. D. Koster, R. J. Suozzo, G. L. Russell, J. W. C. White, and W. S. Broecker, 1991: Simulations of the HDO and $H_2^{18}O$ atmospheric cycles using the NASA GISS General Circulation Model: Sensitivity experiments for present day conditions. *J. Geophys. Res.*, **96**, 7495–7507.
- Kanamitsu, M., W. Ebisuaki, J. Woolen, S. Yang, J. J. Hnilo, M. Fiorino, and G. L. Potter, 2002: NCEP/DOE AMIP-II Re-analysis (R-2). *Bull. Amer. Meteor. Soc.*, **83**, 1631–1643.
- Kistler, R., and Coauthors, 2001: The NCEP–NCAR 50-year reanalysis: Monthly means CD-ROM and documentation. *Bull. Amer. Meteor. Soc.*, **82**, 247–268.

- Liang, X., D. P. Lettenmaier, E. F. Wood, and S. J. Burges, 1994: A simple hydrologically based model of land surface water and energy fluxes for GSMs. *J. Geophys. Res.*, **99** (D7), 14 415–14 428.
- Manabe, S., 1969: Climate and the ocean circulation. I. The atmospheric circulation and the hydrology of the earth's surface. *Mon. Wea. Rev.*, **97**, 739–774.
- Martinelli, L. A., cited 2003: Data submitted to the project for isotope tracing of hydrological processes in large river basins. [Available online at <http://isohis.iaea.org>.]
- Matsui, E., E. Salati, M. N. G. Ribeiro, C. M. Reis, A. C. S. N. F. Tancredi, and J. R. Gat, 1983: Precipitation in the central Amazon basin: The isotopic composition of rain and atmospheric moisture at Belem and Manaus. *Acta Amazonica*, **13**, 307–369.
- McGuffie, K., and A. Henderson-Sellers, 2004: *A Climate Modelling Primer*. J. Wiley and Sons, 310 pp.
- Merlivat, L., and J. Jouzel, 1979: Global climatic interpretation of the deuterium–oxygen 18 relationship for precipitation. *J. Geophys. Res.*, **84** (C8), 5029–5033.
- Nijssen, B., R. Schnur, and D. P. Lettenmaier, 2001: Global retrospective estimation of soil moisture using the variable infiltration capacity land surface model, 1980–93. *J. Climate*, **14**, 1790–1808.
- Noone, D., and I. Simmonds, 1998: Implications for the interpretation of ice-core isotope data from analysis of modelled Antarctic precipitation. *Ann. Glaciol.*, **28**, 398–402.
- , and —, 2002: Association between $\delta^{18}\text{O}$ of water and climate parameters in a simulation of atmospheric circulation for 1979–95. *J. Climate*, **15**, 3150–3169.
- , C. Still, and W. Riley, 2002: A global biophysical model of ^{18}O in terrestrial water and CO_2 fluxes. Research Activities in Atmospheric and Oceanic Modelling, Rep. 32, World Meteorological Organization, Geneva, Switzerland, 4.19–4.20.
- Petit, J. R., and Coauthors, 1999: Climate and atmospheric history of the past 420 000 years from the Vostok ice core, Antarctica. *Nature*, **399**, 429–436.
- Peylin, P., P. Ciais, A. S. Denning, P. P. Tans, J. A. Berry, and J. W. C. White, 1999: A 3-dimensional study of delta O18 in atmospheric CO_2 : Contribution of different land ecosystems. *Tellus*, **51B**, 642–667.
- Randall, D. A., Ed., 2000: *General Circulation Model Development: Past, Present, and Future*. Academic Press, 807 pp.
- Riley, W. J., C. J. Still, M. S. Torn, and J. A. Berry, 2002: A mechanistic model of H_2^{18}O and C^{18}O fluxes between ecosystems and the atmosphere: Model description and sensitivity analyses. *Global Biogeochem. Cycles*, **16**, 1095, doi:10.1029/2002GB001878.
- , —, B. R. Helliker, M. Ribas-Carbo, and J. A. Berry, 2003: ^{18}O composition of CO_2 and H_2O ecosystem pools and fluxes in a tallgrass prairie: Simulations and comparisons to measurements. *Global Change Biol.*, **9**, 1–15.
- Rozanski, K., L. Araguas-Araguas, and R. Gonfiantini, 1993: Isotopic patterns in modern global precipitation. *Climate Change in Continental Isotopic Records*, *Geophys. Monogr.*, No. 78, Amer. Geophys. Union, 1–36.
- Salati, E., and P. B. Vose, 1984: Amazon Basin: A system in equilibrium. *Science*, **225**, 129–137.
- , A. D. Olio, E. Matsui, and J. R. Gat, 1979: Recycling of water in the Amazon basin: An isotopic study. *Water. Resour. Res.*, **15**, 1250–1258.
- Schlosser, C. A., and Coauthors, 2000: Simulations of a boreal grassland hydrology at Valdai, Russia: PILPS Phase 2(d). *Mon. Wea. Rev.*, **128**, 301–321.
- Sellers, P. J., Y. Mintz, Y. C. Sud, and A. Dalcher, 1986: A Simplified Biosphere Model (SiB) for use within general circulation models. *J. Atmos. Sci.*, **43**, 505–531.
- Stone, D. W., A. Henderson-Sellers, P. Airey, and K. McGuffie, 2003: Murray–Darling basin isotope observations: An essential component of the Australian CEOP. *Eos, Trans. Amer. Geophys. Union*, **84** (Fall Meeting Suppl.), H221-08.
- Wood, E. F., and Coauthors, 1998: The Project for Intercomparison of Land-surface Parameterization Schemes (PILPS) Phase 2(c) Red–Arkansas river basin experiment: 1. Experiment description and summary intercomparisons. *Global Planet. Change*, **19**, 115–135.
- Xie, P. P., and P. A. Arkin, 1997: Global precipitation: A 17-year monthly analysis based on gauge observations, satellite estimates, and numerical model outputs. *Bull. Amer. Meteor. Soc.*, **78**, 2539–2558.
- Yang, Z.-L., R. E. Dickinson, A. Henderson-Sellers, and A. J. Pitman, 1995: Preliminary study of spin-up processes in land surface models with the first stage data of Project for Intercomparison of Land Surface Parameterization Schemes Phase 1(a). *J. Geophys. Res.*, **100** (D8), 16 553–16 578.
- Yonge, C. J., L. Goldenberg, and H. R. Krouse, 1989: An isotope study of water bodies along a traverse of southwestern Canada. *J. Hydrol.*, **106**, 245–255.